PHYSICAL REVIEW D **96,** 034022 (2017)

Phases of circle-compactified QCD with adjoint fermions at finite density

Takuya Kanazawa,[1] Mithat Ünsal,[2] and Naoki Yamamoto[3]
[1]*iTHES Research Group and Quantum Hadron Physics Laboratory, RIKEN, 6-7-1 Minatojima-minamimachi, Chuo-ku, Kobe, Hyogo 650-0047, Japan*
[2]*Department of Physics, North Carolina State University, Raleigh, North Carolina 27695, USA*
[3]*Department of Physics, Keio University, Yokohama 223-8522, Japan*
(Received 28 March 2017; published 25 August 2017)

We study chemical-potential dependence of confinement and mass gap in QCD with adjoint fermions in spacetime with one spatial compact direction. By calculating the one-loop effective potential for the Wilson line in the presence of a chemical potential, we show that a center-symmetric phase and a center-broken phase alternate when the chemical potential in units of the compactification scale is increased. In the center-symmetric phase we use semiclassical methods to show that photons in the magnetic bion plasma acquire a mass gap that grows with the chemical potential as a result of anisotropic interactions between monopole-instantons. For the neutral fermionic sector which remains gapless perturbatively, there are two possibilities at a nonperturbative level: either to remain gapless (unbroken global symmetry) or to undergo a novel superfluid transition through a four-fermion interaction (broken global symmetry). If the latter is the case, this leads to an energy gap of quarks proportional to a new nonperturbative scale $L^{-1}\exp[-1/(g^4\mu L)]$, where L denotes the circumference of S^1, the low-energy physics is described by a Nambu-Goldstone mode associated with the baryon number, and there exists a new type of BEC-BCS crossover of the diquark pairing as a function of the compactification scale at a small chemical potential.

DOI: 10.1103/PhysRevD.96.034022

I. INTRODUCTION

Semiclassical analysis is a powerful tool to study quantum systems nonperturbatively. In QCD, instantons have long been a subject of intensive research [1–4]. They played crucial roles in phenomenological models of spontaneous chiral symmetry breaking, as well as the U(1) problem and the strong CP problem. In dense quark matter, instanton effects are semiclassically reliable as it has been widely recognized [5–11].

Our understanding of semiclassical aspects of non-Abelian gauge theories including QCD was significantly advanced with two related areas of progress:

(i) KvBLL monopole-instantons on $\mathbb{R}^3 \times S^1$ [12–14],
(ii) Semiclassically calculable domains on $\mathbb{R}^3 \times S^1$ in (nonsupersymmetric) QCD-like and Yang-Mills theories [15–17].

Monopole-instantons carry fractional topological charge and obey the Nye-Singer index theorem [18,19] (which is a refinement of the Atiyah-Singer index). The sum of the fermion zero modes of the monopole-instantons is equal to the one of instantons in four dimensions (4d); hence, they are more relevant for chiral symmetry breaking. In sharp contrast to 4d instantons, monopole-instantons on $\mathbb{R}^3 \times S^1$ explicitly depend on the background holonomy (Wilson line) field. Therefore, monopole-instantons provide a concrete connection between center-symmetry realization (confinement in a thermal context) and chiral symmetry realization.

In $\mathcal{N} = 1$ supersymmetric Yang-Mills (SYM) theory on $S^1 \times \mathbb{R}^3$, the ensemble of monopole-instantons generates the gluino condensate [20]. The applicability of semiclassics to nonsupersymmetric QCD-like theories was shown in Refs. [15–17,21–23]. (Also see Ref. [24].) In such theories gauge symmetry "breaking" occurs at small S^1 (at weak coupling) due to the Hosotani mechanism [25]. In SYM as well as in adjoint QCD, in the Abelian regime, topologically neutral molecules of monopoles called "magnetic bions" form and generate a bosonic potential that engenders a mass gap of gluons and confines quarks [15,17].

In this work, we study phases of compactified adjoint QCD on $\mathbb{R}^3 \times S^1$ at nonzero quark chemical potential μ. It should be noted that S^1 in this paper is a compactified *spatial* direction along which fermions obey the periodic boundary condition (PBC); the imaginary-time direction is infinite and the system is at zero temperature. This setup must not be confused with previous studies of a holonomy potential for *thermal* S^1 at $\mu \neq 0$ [26–30].

This theory is weakly coupled at small S^1 for any value of μ.[1] For generic colors (N_c) and Dirac flavors (N_f^{D}) we compute the perturbative one-loop potential for the Wilson line holonomy. We find that turning on a small μ weakens gauge symmetry breaking, while a larger μ induces an infinite number of oscillatory transitions between a gauge-symmetry-restored phase and a broken phase. In the

[1]At large μ and for sizes of S^1 larger than the strong length scale, there are subsectors of the theory amenable to the weak coupling treatment; however, there are sectors of the theory which are still strongly coupled, in particular, the gauge sector.

specific case of $N_c = 2$ and $N_f^{\mathrm{D}} = 1$, we show that perturbatively induced four-fermion operators[2] that have so far been neglected in studies of the Hosotani phase can play a pivotal role in generating diquark condensation and drive the system into a superfluid phase with broken $\mathrm{U}(1)_B$ baryon number symmetry. Our calculations are performed in a theoretically controlled setting thanks to the small running coupling and complete Abelianization of the gauge group at small S^1. This is a unique opportunity in which one can derive both continuous symmetry breaking and confinement from first principles analytically, providing a valuable laboratory to study the strongly coupled QCD vacuum.

As a quick guide to readers, we summarize a cascade of symmetry breaking in the presence of μ for $N_c = 2$ and $N_f^{\mathrm{D}} = 1$ when μ is small compared to the compactification scale L^{-1}:

$$\mathrm{U}(2)_f \times [\mathrm{SU}(2)]_c \tag{1}$$

$$\xrightarrow{\text{anomaly}} ((\mathbb{Z}_8)_A \times \mathrm{SU}(2)_f)/\mathbb{Z}_2 \times [\mathrm{SU}(2)]_c \tag{2}$$

$$\xrightarrow{\mu \neq 0} ((\mathbb{Z}_8)_A \times \mathrm{U}(1)_B)/\mathbb{Z}_2 \times [\mathrm{SU}(2)]_c \tag{3}$$

$$\xrightarrow{\text{Adj Higgs}} ((\mathbb{Z}_8)_A \times \mathrm{U}(1)_B)/\mathbb{Z}_2 \times [\mathrm{U}(1)]_c \tag{4}$$

$$\xrightarrow{\langle\chi\rangle=0,\pi} ((\mathbb{Z}_4)_A \times \mathrm{U}(1)_B)/\mathbb{Z}_2 \times [\mathrm{U}(1)]_c \tag{5}$$

$$\xrightarrow{\langle\psi\psi\rangle\neq 0} (\mathbb{Z}_2)_R \times (\mathbb{Z}_2)_L \times [\mathrm{U}(1)]_c. \tag{6}$$

Here $[...]_c$ denotes the unbroken part of the gauge group and χ is the dual photon field. In (2)–(5) we have factored a common $\mathbb{Z}_2$ group to avoid double counting. Detailed explanations will follow later.

In Fig. 1 we present a schematic phase diagram of adjoint QCD with the aim to illustrate how our analysis in this paper in the small-S^1 regime should fit in the global phase diagram from small to large S^1. Adjoint QCD on $\mathbb{R}^4$ is believed to exhibit a relativistic analogue of the BEC-BCS crossover [31,32] when the chemical potential is swept across Λ_{QCD} [33–41]:

(i) At $\mu = 0$ and large L, the center symmetry is preserved, while the flavor symmetry is believed to be spontaneously broken as $\mathrm{SU}(2)_f \to \mathrm{SO}(2)_f$ for $N_f^{\mathrm{D}} = 1$ [42]. The physical spectrum contains a light diquark that undergoes a Bose condensation for $\mu > m_\pi/2$ and breaks $\mathrm{U}(1)_B$. This onset of superfluidity is well described by chiral perturbation theory [33].

(ii) In the asymptotic region $\mu \gg \Lambda_{\mathrm{QCD}}$, on $\mathbb{R}^4$, quarks acquire a large energy gap $\Delta \sim \mu e^{-1/g}$ from the perturbative one-gluon exchange at the Fermi surface [43,44] and the low-energy effective theory is anisotropic Yang-Mills theory with a confining scale Λ' that goes down to zero as $\mu \to \infty$ due to medium effects [45]. The compactification $L < \infty$ acts on gluons as a thermal scale and triggers a deconfinement transition at $L^{-1} \sim \Lambda'$. This is why the phase transition line must emanate from the top right corner of the phase diagram in Fig. 1.

(iii) At $\mu = 0$, if $L\Lambda_{\mathrm{QCD}} \ll 1$, the system enters a center-symmetric weakly coupled regime where the discrete chiral symmetry remains broken, while the continuous chiral symmetry is restored [15]. This is indicated by a red line in the bottom left corner of Fig. 1.

(iv) The above three domains are well understood by now. In this paper, we venture into the novel regime of small S^1 and any μ. Among other things we uncover, in addition to a series of confinement-deconfinement transitions, we find that a novel mechanism which can engender superfluidity even for *arbitrarily small* L and μ, as long as $\mu \neq 0$, is a logical possibility. The condition under which this possibility may be realized will be carefully examined later. The estimated nonperturbative gap of quarks is of order $\Delta \sim L^{-1} e^{-1/(g^4 \mu L)}$.[3]

Now, if the adiabatic continuity of center symmetry at $\mu = 0$ from small to large S^1 (conjectured in Refs. [15–17] and tested numerically in Refs. [47,48]) holds, then it follows that a *double crossover* should emerge on the phase diagram (Fig. 1), uniting two weakly coupled BCS superfluids: one at small S^1 and the other at large S^1 and $\mu \gg \Lambda_{\mathrm{QCD}}$. It is highly nontrivial that such a continuity may exist, because the two phases have distinct physical mechanisms for quark pairing: two-charged-boson exchange interaction on one hand (at small S^1; see Fig. 12 below) and the one-gluon-exchange interaction on the other hand.

This paper is organized as follows. In Sec. II we examine the perturbative holonomy potential and reveal a complex phase diagram at $\mu \neq 0$ and nonzero masses for $N_c = 2$ and 3. The quark number density is also computed. In Sec. III we analyze how the monopole-binding interaction due to fermion-zero-mode exchange is modified at $\mu \neq 0$. It is

[2]The monopole operators which also possess four fermionic zero modes are nonperturbatively weak in the semiclassical domain.

[3]It is intriguing to draw a comparison between dense QCD, the Nambu–Jona-Lasinio (NJL) model, and our case. In dense QCD the gap is $\sim e^{-1/g}$ due to unscreened magnetic gluons [43]. In the NJL-type model with a pointlike four-fermion interaction, the gap is generally $\sim e^{-1/g^2}$ [46]. The dependence e^{-1/g^4} found in this work differs from either of them.

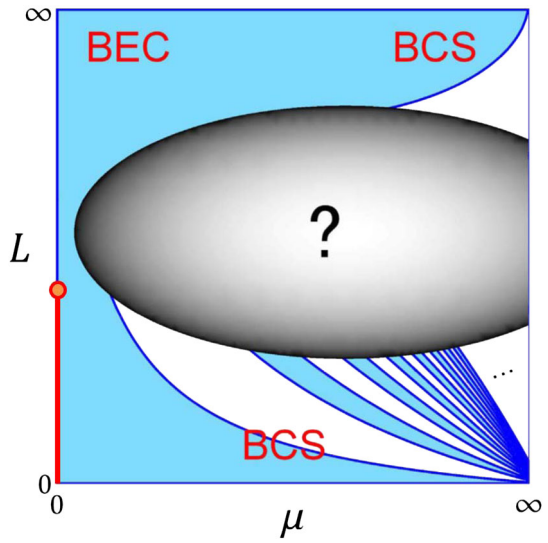

FIG. 1. Phase diagram of $N_c = 2$ adjoint QCD on $\mathbb{R}^3 \times S^1$ in the chiral limit based on the result of our investigation, with L the circumference of S^1. The blue region represents the center-symmetric phase and the white region the center-broken phase. The diquark condensate $\langle\psi\psi\rangle$ vanishes on the $L \lesssim \Lambda_{\rm QCD}^{-1}$ part of the L axis (represented by a red line with a critical end point). The weakly coupled superfluid phase at small L labeled as "BCS" relies on the assumption that the four-quark interaction induced in the center-symmetric phase has an attractive channel (see Sec. III C for more details). The phase structure at intermediate L is currently unknown.

shown for $N_c = 2$ that the chemical potential renders the intermonopole potential strongly anisotropic, favoring a temporal separation. A fermionic low-energy effective theory is also examined and the conditions under which spontaneous $\mathrm{U}(1)_B$ breaking occurs at an arbitrarily small chemical potential are derived. The fermion gap Δ is shown to be proportional to $e^{-1/(g^4\mu L)}$, which is smaller than any finite order of the semiclassical expansion in powers of $e^{-S_{\rm m}}$ where $S_{\rm m} = 8\pi^2/(g^2 N_c) = 4\pi^2/g^2$. The effective Lagrangian of the Nambu-Goldstone mode associated with the $\mathrm{U}(1)_B$ breaking is also derived. We conclude in Sec. IV. Technical details on the derivation of the perturbative potential and properties of a free fermion propagator at $\mu \neq 0$ are summarized in Appendixes A and B, respectively.

II. HOSOTANI MECHANISM WITH CHEMICAL POTENTIAL

We consider $\mathrm{SU}(N_c)$ gauge theory on $\mathbb{R}^3 \times S^1$ with $N_f^{\rm D}$ flavors of four-component Dirac fermions $\Psi_f = \Psi_f^{\mathsf{A}} t^{\mathsf{A}}$ in the adjoint representation, obeying PBC on S^1. We will use $f, g, \ldots$ to label flavors $\{1, 2, \ldots, N_f^{\rm D}\}$ and $\mathsf{A}, \mathsf{B}, \ldots$ to label the adjoint colors $\{1, 2, \ldots, N_c^2 - 1\}$. (The fundamental colors $\{1, 2, \ldots, N_c\}$ will be labeled by $\mathrm{a}, \mathrm{b}, \ldots$.) The generators are normalized as $\mathrm{tr}(t^{\mathsf{A}} t^{\mathsf{B}}) = \delta^{\mathsf{AB}}/2$. The circumference of S^1 is denoted by L. The asymptotic freedom requires $N_f^{\rm D} < 2.75$ and this is hereafter assumed unless stated otherwise. The Lagrangian reads

$$\mathcal{L} = \mathrm{tr}\left\{\frac{1}{2g^2} F_{\alpha\beta}^2 + 2\overline{\Psi}_f [\not{D}(\mu) + m]\Psi_f\right\}, \tag{7}$$

where $F_{\alpha\beta} = F_{\alpha\beta}^{\mathsf{A}} t^{\mathsf{A}}$ and $\not{D}(\mu) = \not{D} - \mu\gamma_4$. In this paper we will always work in Euclidean spacetime, using $\alpha, \beta, \ldots$ to denote the entire four directions $\{1, 2, 3, 4\}$ while reserving $i, j, \ldots$ for noncompact directions $\{1, 2, 4\}$ only. The compactified spatial direction is x^3 in our setting.

For $N_f^{\rm D} \geq 1$ and $\mu = 0$ the gauge symmetry is known to be dynamically broken to the maximal torus $\mathrm{U}(1)^{N_c-1}$ by quantum effects of periodic fermions if both $L\Lambda_{\rm QCD}$ and Lm are sufficiently small [15,25,49]. In this section we examine how the chemical potential term $\mu\Psi^\dagger\Psi$ influences gauge symmetry breaking at small S^1, putting aside the issue of photon mass gap and fermion bilinear condensation. This treatment is justified because the latter effects are nonperturbatively small while gauge symmetry is broken at one loop.

A. Perturbative potential for the Wilson line

We consider a uniform background gauge field that is zero in $\mathbb{R}^3$ directions and nonvanishing along S^1. The holonomy is given by

$$\Omega \equiv \mathcal{P}\exp\left(i\oint \mathrm{d}x^3 A_3\right). \tag{8}$$

We employ the gauge in which Ω is diagonal,

$$A_3 = \mathrm{diag}(a_1, a_2, \ldots, a_{N_c}), \qquad \sum_{\mathrm{a}=1}^{N_c} a_{\mathrm{a}} = 0, \tag{9}$$

and define dimensionless variables for later convenience:

$$\hat{\mu} \equiv L\mu, \qquad \hat{m} \equiv Lm, \quad \text{and} \quad \hat{a}_{\mathrm{a}} \equiv L a_{\mathrm{a}}. \tag{10}$$

The object to be calculated is the one-loop effective potential for the holonomy at $\mu \neq 0$. It consists of several pieces,

$$V(\Omega;\mu) = V_{\rm YM}(\Omega) + N_f^{\rm D}[V_{\rm F}(\Omega) + \delta V_{\rm F}(\Omega;\mu)]. \tag{11}$$

The first term is the contribution of the gauge fields and ghosts [1],

$$V_{\rm YM}(\Omega) = \frac{1}{24\pi^2 L^4}\sum_{\mathrm{a},\mathrm{b}=1}^{N_c} F_1(\hat{a}_{\mathrm{a}} - \hat{a}_{\mathrm{b}}), \tag{12}$$

with $F_1(\hat{a}) \equiv [\hat{a}]^2(2\pi - [\hat{a}])^2$, where $0 \le [\hat{a}] \le 2\pi$ is equal to $\hat{a}$ mod 2π. $V_{\rm F}(\Omega)$ is the potential induced by a single adjoint Dirac fermion with PBC at $\mu = 0$ [49,50],

$$V_{\rm F}(\Omega) = \frac{2\hat{m}^2}{\pi^2 L^4}\sum_{n=1}^{\infty}\frac{1}{n^2}|\mathrm{tr}\,\Omega^n|^2 K_2(n\hat{m}) = \frac{2}{\pi^2 L^4}\sum_{\mathsf{a},\mathsf{b}=1}^{N_c} F_2(\hat{m}, \hat{a}_{\mathsf{a}} - \hat{a}_{\mathsf{b}}), \tag{13}$$

with

$$F_2(\hat{m}, \hat{a}) \equiv \hat{m}^2 \sum_{n=1}^{\infty}\frac{1}{n^2}K_2(n\hat{m})\cos(n\hat{a}). \tag{14}$$

What remains is to compute $\delta V_{\rm F}(\Omega;\mu)$, which controls the μ dependence of the effective potential. In terms of the quark determinant

$$\Gamma_q(\Omega;\mu) \equiv \log\det[\not{D}(\mu) + m], \tag{15}$$

we have

$$\delta V_{\rm F}(\Omega;\mu) = -\frac{1}{V_{\mathbb{R}^3}L}\{\Gamma_q(\Omega;\mu) - \Gamma_q(\Omega;0)\}, \tag{16}$$

where $V_{\mathbb{R}^3}$ formally denotes the infinite volume of the spacetime in $x^{1,2,4}$ directions. Technical details of the evaluation of Γ_q are given in Appendix A. The result is

$$\delta V_{\rm F}(\Omega;\mu) = -\frac{1}{2\pi L^4}\left\{\sum_{\mathsf{a},\mathsf{b}=1}^{N_c} F_3(\hat{\mu}, \hat{m}, \hat{a}_{\mathsf{a}} - \hat{a}_{\mathsf{b}}) - F_3(\hat{\mu}, \hat{m}, 0)\right\}, \tag{17}$$

with

$$F_3(\hat{\mu}, \hat{m}, \hat{a}) \equiv \sum_{n=-\infty}^{\infty}\theta(\hat{\mu}^2 - \hat{m}^2 - (\hat{a} + 2n\pi)^2) \times \left[\frac{1}{3}\hat{\mu}^3 - \hat{\mu}\{(\hat{a} + 2n\pi)^2 + \hat{m}^2\} + \frac{2}{3}\{(\hat{a} + 2n\pi)^2 + \hat{m}^2\}^{3/2}\right], \tag{18}$$

where $\theta(x)$ is the Heaviside step function. It is immediately clear from (18) that $\delta V_{\rm F}(\Omega;\mu)$ vanishes when $\mu < m$. This is expected because μ below the energy gap (mass of adjoint fermion) has no physical effect at zero temperature.

Collecting (11), (12), (13), and (17), we obtain the one-loop effective potential. Next we proceed to numerical analysis of the phase diagram for $N_c = 2$ and 3 based on minimization of $V(\Omega;\mu)$.

TABLE I. Phases for $N_c = 2$.

Minimum	$\mathbb{Z}_2$ center	Gauge symmetry
$\hat{a} = 0, \pi$	Broken	SU(2)
$\hat{a} = \pi/2$	Unbroken	U(1)

B. $N_c = 2$

For $N_c = 2$ the holonomy can be parametrized as $\Omega = \mathrm{diag}(e^{i\hat{a}}, e^{-i\hat{a}})$. In numerical minimization of the potential $V(\Omega;\mu)$ we encounter the two phases in Table I. Let us summarize the bosonic spectrum in each phase.

(i) In the first phase with broken center symmetry, the A_3 component of gluons acquires a mass of $\mathcal{O}(g/L)$ (called the electric screening mass in the case of thermal S^1) while the other components $A_{1,2,4}$ are perturbatively massless and interact strongly with periodic fermions. In the limit $L \to 0$ with fixed μ, the system would reduce to three-dimensional adjoint QCD at finite μ.

(ii) The second phase entails Abelianization of the gauge group due to the Hosotani mechanism. Similarly to W bosons in the electroweak theory, $A_{1,2,4}^{\mathsf{A}=1,2}$ acquire a mass $m_{\rm W} = \pi/L$ by eating $A_3^{\mathsf{A}=1,2}$; the "Higgs mode" $A_3^{\mathsf{A}=3}$ gains a mass $m_{\rm H} \sim g/L$; and the photons $A_{1,2,4}^{\mathsf{A}=3}$ are massless to all orders in perturbation theory.

In Fig. 2 the holonomy potential for $N_f^{\rm D} = 1$ in the chiral limit is plotted. As $\hat{\mu}$ increases, the center-symmetric phase is turned into a center-broken phase via a first-order transition. Namely μ counteracts the Hosotani mechanism in this parameter range.[4] To explain why, let us look at the quark number density

$$n_q \equiv -N_f^{\rm D}\frac{\partial}{\partial\mu}\delta V_{\rm F}(\Omega;\mu) = \frac{N_f^{\rm D}}{2\pi L^3}\{2F_3'(\hat{\mu}, \hat{m}, 2\hat{a}) + F_3'(\hat{\mu}, \hat{m}, 0)\}, \tag{19}$$

with

$$F_3'(\hat{\mu}, \hat{m}, \hat{a}) = \sum_{n=-\infty}^{\infty}\{\hat{\mu}^2 - \hat{m}^2 - (\hat{a} + 2n\pi)^2\} \times \theta(\hat{\mu}^2 - \hat{m}^2 - (\hat{a} + 2n\pi)^2). \tag{20}$$

The first term in (19) represents the density of $\Psi^{\mathsf{A}=1,2}$, which are charged under the unbroken U(1) gauge symmetry. The second term in (19) represents the density of neutral fermions $\Psi^{\mathsf{A}=3}$; since it does not depend on the holonomy it can be ignored for the moment.

As (20) implies, due to compactification, the Fermi sea becomes a union of multiple disks in momentum space, labeled as

[4]This is in contrast with the case of an external magnetic field [51], which *enlarges* the center-symmetric phase.

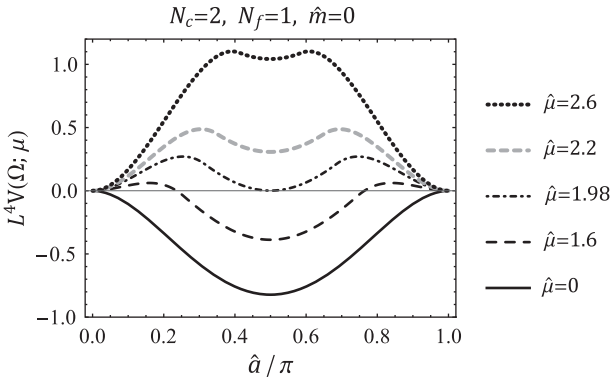

FIG. 2. Effective potential for $N_c = 2$ and $N_f^{\mathrm{D}} = 1$ in the chiral limit. In this figure, V is normalized to 0 at $\hat{a} = 0$.

$$\mathrm{KK}_\ell \equiv \left\{ (p_1, p_2, p_3) \middle| p_3 = \frac{\ell\pi}{L}, \sqrt{\boldsymbol{p}^2 + m^2} \le \mu \right\} \tag{21}$$

with $\ell \in \mathbb{Z}$. (Precisely speaking, this p_3 is the eigenvalue of $i\partial_3 + A_3$ rather than $i\partial_3$.) Such a discrete structure of energy levels is analogous to the Landau levels in a magnetic field. As shown in Fig. 3, charged fermions occupy either $\mathrm{KK}_{\ell=\mathrm{even}}$ or $\mathrm{KK}_{\ell=\mathrm{odd}}$ with $|\ell| \le \sqrt{\hat{\mu}^2 - \hat{m}^2}/\pi$ depending on the holonomy. Namely, in the center-symmetric phase ($\hat{a} = \pi/2$) the holonomy dynamically changes the boundary condition of charged fermions along S^1 from periodic to *antiperiodic*. We note that every time μ reaches a new KK_ℓ level, a second-order phase transition occurs; the quark number susceptibility jumps. Indeed there are an infinite number of second-order transitions as a function of μ.[5]

Let us examine what happens at small $\hat{\mu}$. When $\hat{m} \le \hat{\mu} < \sqrt{\pi^2 + \hat{m}^2}$, μ lies between KK_0 and $\mathrm{KK}_{\pm1}$. Hence KK_0 forms the charged Fermi sea in the center-broken phase. On the other hand, no Fermi sea exists yet in the center-symmetric phase. This means that the pressure in the center-broken phase is higher, by the amount of the degenerate Fermi sea, implying that center symmetry breaking is favored by $\delta V_{\mathrm{F}}(\Omega;\mu)$ for $\hat{\mu}$ in this range. This explains the first-order transition in Fig. 2.

Interestingly, this is not the whole story. As $\hat{\mu}$ increases further, many KK_ℓ join the Fermi sea and the competition between $\mathrm{KK}_{\ell=\mathrm{even}}$ and $\mathrm{KK}_{\ell=\mathrm{odd}}$ becomes quite subtle. In Fig. 4 we plot the difference of F_3, (18), in the two vacua at $\hat{m} = 0$. It shows a growing oscillation in $\hat{\mu}$ with period $\approx 2\pi$. At small $\hat{\mu}$ the oscillation starts with a negative value, implying that the center-broken vacuum is favored by medium. As $\hat{\mu}$ increases, however, the zero is crossed infinitely many times and consequently it leads to an endless alternation of the two vacua. In Fig. 5 we show the phase diagram of center symmetry, showing the presence of infinitely many center-symmetric phases.[6] One can tune $\hat{\mu}$ to bring the system into a center-symmetric phase, however large the mass $\hat{m}$.

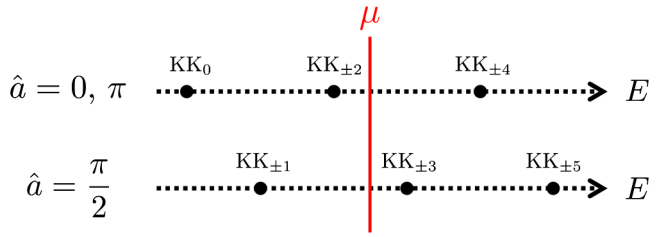

FIG. 3. The structure of KK_ℓ energy levels for the center-broken ($\hat{a} = 0, \pi$) and center-symmetric ($\hat{a} = \pi/2$) phases. In this example, the Fermi sea of charged fermions consists of $\mathrm{KK}_0 \cup \mathrm{KK}_{\pm2}$ or $\mathrm{KK}_{\pm1}$, depending on the holonomy.

It should be noted that the center-symmetric phases at $\hat{\mu} > 1$ are different from the well-studied center-symmetric phase at $\hat{m} \sim \hat{\mu} \sim 0$ in that there is a Fermi sea of charged fermions $\Psi^{\mathsf{A}=1,2}$ in the former but not in the latter.

The stripe structure of the phase diagram in Fig. 5 is reflected in the μ dependence of other observables as well. Figure 6 plots the quark density n_q (divided by μ^2 to make the stratified structure clearer). The lines of center-symmetry-changing first-order transitions are clearly visible. In addition, m_{H} (the mass of $A_3^{\mathsf{A}=3}$) oscillates with $\hat{\mu}$, but it stays at $\mathcal{O}(g/L)$ and never vanishes because the transitions are first order.

C. $N_c = 3$

For $N_c = 3$ the holonomy can be parametrized as $\Omega = \mathrm{diag}(e^{i\hat{a}_1}, e^{i\hat{a}_2}, e^{-i(\hat{a}_1+\hat{a}_2)})$. In numerical minimization of the potential $V(\Omega;\mu)$ with respect to $\hat{a}_1$ and $\hat{a}_2$ we found three phases in Table II. The phase in the second row, often called the *split* (or *skewed*) phase, was found in Ref. [53] in a deformed SU(3) Yang-Mills theory and has been studied in a variety of setups [27,47,48,54]. The other two phases are natural generalizations of those for $N_c = 2$.

As for $N_c = 2$, we again find that the addition of $\hat{\mu}$ destabilizes the center-symmetric vacuum realized at $\hat{\mu} = 0$. Figure 7 displays the evolution of the holonomy potential for increasing $\hat{\mu}$. We observe that each phase in the above table is realized successively (from bottom to top) for increasing $\hat{\mu}$. An explanation in terms of KK_ℓ levels becomes rather cumbersome and is not as useful as for SU(2).

When $\hat{\mu}$ is further increased, the three phases periodically alternate and there are an infinite number of first-order

[5]This phenomenon, analogous to the de Haas–van Alphen effect in solid state physics, has been studied in NJL models with spatial compactification [52].

[6]A similar phase structure was observed in QCD on $S^1 \times S^3$ with nonzero chemical potential [28].

TABLE II. Phases for $N_c = 3$.

$(\hat{a}_1, \hat{a}_2)$ at the minimum	$\mathbb{Z}_3$ center	Gauge symmetry
$(0, 0)$, $\pm(\frac{2\pi}{3}, \frac{2\pi}{3})$	Broken	SU(3)
$\pm(\frac{\pi}{3}, \frac{\pi}{3})$, $\pm(\frac{\pi}{3}, -\frac{2\pi}{3})$, $\pm(-\frac{2\pi}{3}, \frac{\pi}{3})$	Broken	$\mathrm{SU}(2) \times \mathrm{U}(1)$
$(0, \pm\frac{2\pi}{3})$, $(\pm\frac{2\pi}{3}, \mp\frac{2\pi}{3})$, $(\pm\frac{2\pi}{3}, 0)$	Unbroken	$\mathrm{U}(1) \times \mathrm{U}(1)$

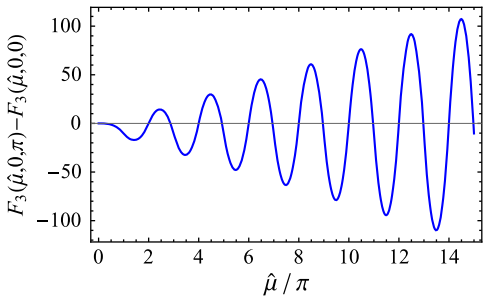

FIG. 4. Difference of the free energy with a center-symmetric vs center-broken holonomy in the massless limit [with F_3 defined in (18)].

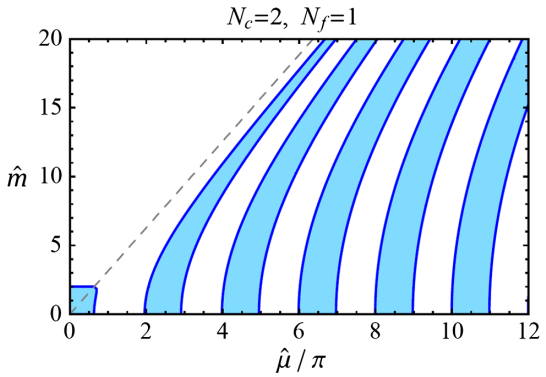

FIG. 5. Phase diagram of center symmetry for $N_c = 2$ and $N_f^{\mathrm{D}} = 1$. The shaded (empty) region is a center-symmetric (center-broken) phase, respectively. They are separated by first-order transitions. The dashed line represents $\hat{m} = \hat{\mu}$.

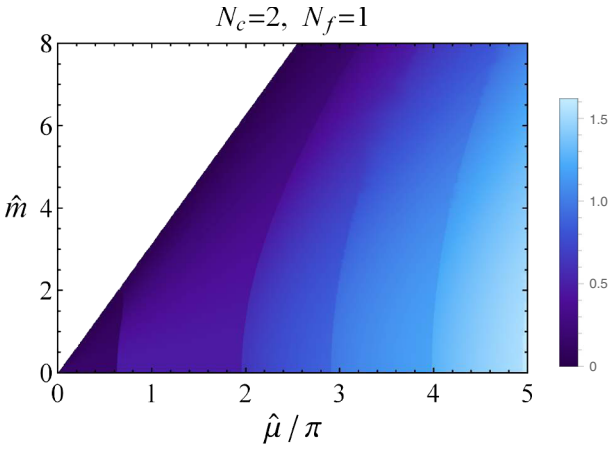

FIG. 6. The rescaled quark number density Ln_q/μ^2 for $N_c = 2$ and $N_f^{\mathrm{D}} = 1$. The $\hat{m} > \hat{\mu}$ region where the density is strictly zero is left empty.

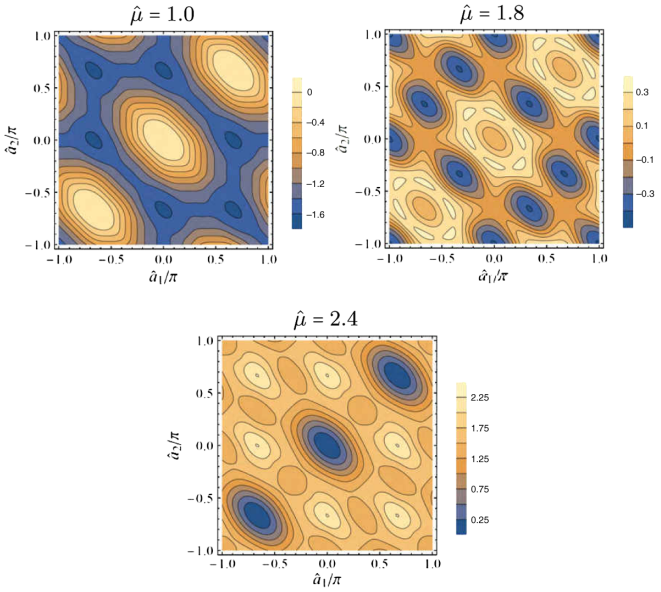

FIG. 7. Effective potential $L^4 V(\Omega;\mu)$ for $N_c = 3$ and $N_f^{\mathrm{D}} = 1$ in the chiral limit, normalized to 0 at $\hat{a}_1 = \hat{a}_2 = 0$. Each $\hat{\mu}$ corresponds to the three different phases (see the main text and Fig. 8). First-order phase transitions occur at $\hat{\mu} = 1.42$ and $\hat{\mu} = 1.98$.

transitions. The phase diagram for $N_f^{\mathrm{D}} = 1$ is displayed in Fig. 8. Again we find that a center-symmetric phase can be realized for an *arbitrarily large* fermion mass by tuning μ judiciously. The global features of Fig. 8 are similar to Fig. 5 except for the presence of the split phase. The quark density n_q/μ^2 is plotted in Fig. 9. It increases monotonically with $\hat{\mu}$ and exhibits tiny jumps along the first-order transition lines in Fig. 8.

It is tempting to conjecture that, as we increase N_c, the phase diagram will contain a variety of more exotic phases

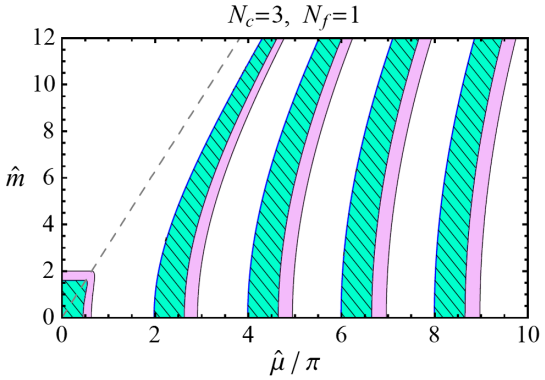

FIG. 8. Phase diagram for $N_c = 3$ and $N_f^{\mathrm{D}} = 1$. The hatched region is the $\mathrm{U}(1) \times \mathrm{U}(1)$ center-symmetric phase, the shaded region is the $\mathrm{SU}(2) \times \mathrm{U}(1)$ split phase, and the empty region is the SU(3) center-broken phase. The phase boundaries are first order. The dashed line represents $\hat{m} = \hat{\mu}$.

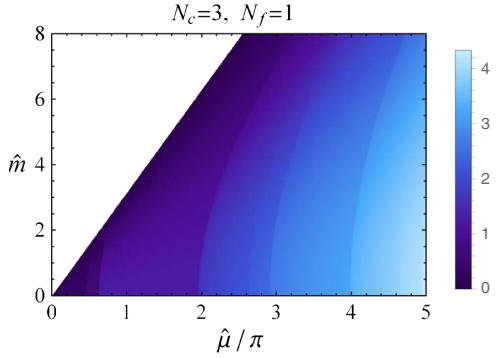

FIG. 9. The rescaled quark number density Ln_q/μ^2 for $N_c = 3$ and $N_f^{\mathrm{D}} = 1$. The $\hat{m} > \hat{\mu}$ region where the density is strictly zero is left empty.

with partial center symmetry breaking, such as those found in Refs. [27,49,55]. However, when L is made larger, all such center-breaking phases must somehow disappear because adjoint QCD on $\mathbb{R}^4$ is a strongly coupled confining theory (cf. Fig. 1). Although revealing the phase structure at intermediate L is beyond the realm of the weak-coupling method in this paper, this can be studied in lattice simulations in principle as the path-integral measure of adjoint QCD is positive semidefinite even at $\mu \neq 0$ [56].

III. LOW-ENERGY EFFECTIVE THEORY AND SYMMETRY BREAKING

A. General discussion

In the previous section we have shown by using the one-loop effective potential of holonomy that there are three phases (below we assume $N_c = 2$ for simplicity):

(i) Phase I: Center-broken phase with $\Omega = \pm\mathbb{1}_2$
(ii) Phase II: Center-symmetric phase at $\hat{\mu} > \pi$
(iii) Phase III: Center-symmetric phase at $\hat{\mu} < \pi$ (the small square next to the origin in Fig. 5)

Phases II and III are similar in terms of center symmetry, but it is useful to distinguish them for later purposes. In the following, we aim to analyze the low-energy dynamics in each phase, with a focus on Phase III. Before doing so, it may be useful to remind global symmetries of adjoint QCD as it has unique features that are absent in ordinary QCD. The classical massless Lagrangian of this theory with N_f^{D} Dirac flavors at $\mu = 0$ is invariant under $\mathrm{U}(1)_A \times \mathrm{SU}(2N_f^{\mathrm{D}})$ symmetry due to the reality of the adjoint representation [42,57], with $\mathrm{U}(1)_B \subset \mathrm{SU}(2N_f^{\mathrm{D}})$ the baryon number symmetry acting as $\Psi \to e^{i\varphi}\Psi$. Chiral anomaly reduces $\mathrm{U}(1)_A$ down to $\mathbb{Z}_{4N_cN_f^{\mathrm{D}}}$. In $\mathbb{R}^4$ (i.e., $L \to \infty$), if N_f^{D} is below the conformal window, the continuous part of the flavor symmetry will be spontaneously broken by the chiral condensate $\langle \mathrm{tr}\overline{\Psi}\Psi\rangle \neq 0$ as $\mathrm{SU}(2N_f^{\mathrm{D}}) \to \mathrm{SO}(2N_f^{\mathrm{D}})$ [42,57]. The chemical potential $\mu \neq 0$ spoils the symmetry between fermions and antifermions and breaks the flavor symmetry explicitly as $\mathrm{SU}(2N_f^{\mathrm{D}}) \to \mathrm{U}(1)_B \times \mathrm{SU}(N_f^{\mathrm{D}})_L \times \mathrm{SU}(N_f^{\mathrm{D}})_R$ for $N_f^{\mathrm{D}} \geq 2$ and $\mathrm{SU}(2N_f^{\mathrm{D}}) \to \mathrm{U}(1)_B$ for $N_f^{\mathrm{D}} = 1$ [33]. From here on, we will focus our attention on the minimal $N_f^{\mathrm{D}} = 1$ case, so that the nonanomalous global symmetry that can be spontaneously broken at $\mu \neq 0$ is $(\mathbb{Z}_8)_A \times \mathrm{U}(1)_B$, as noted earlier in (3).

Let us begin with Phase I in the list above. This phase, having intact SU(2) gauge symmetry, bears similarity to the deconfined phase of thermal QCD, except that fermions obey PBC along S^1 here. In the limit $L \to 0$ all modes other than KK_0 will decouple and we end up with adjoint QCD in $\mathbb{R}^3$ with μ, with a dimensionful coupling[7]

$$g_3^2 \equiv \frac{g^2}{L}. \tag{22}$$

This is a strongly coupled theory and not amenable to semiclassical analysis, but we can guess the physics qualitatively. Because there is a nonzero density of fermions for $\mu > m$ and there is an attractive channel in the color interaction mediated by SU(2) gluons, the BCS mechanism will most likely trigger diquark condensation $\langle \mathrm{tr}\Psi^{\mathrm{T}}\Psi\rangle$ that breaks $\mathrm{U}(1)_B$ spontaneously and generates a pairing gap for fermions. While this scenario sounds plausible, a serious study must incorporate the pairing of fermions and the nonperturbative mass gap of gluons simultaneously. This is an interesting open problem.

Next we consider Phase II. At energy scales far below $m_{\mathrm{W}} = \pi/L$ and $m_{\mathrm{H}} = \mathcal{O}(g/L)$, one can adopt a description in terms of compact U(1) gauge theory with fermions Ψ. At $\mu = 0$, charged fermions $\Psi^{\pm} \equiv (\Psi^{\mathsf{A}=1} \pm i\Psi^{\mathsf{A}=2})/\sqrt{2}$ can also be integrated out due to their large "screening mass" π/L [15]. However, at $\mu > \sqrt{(\pi/L)^2 + m^2}$ (or $\hat{\mu} > \pi$ in the chiral limit), there is a Fermi surface of $\Psi^{\pm}$ on top of that of neutral $\Psi^{\mathsf{A}=3}$, so the charged fermions cannot be dropped from the long-distance effective description.[8] The attractive Coulomb interaction between Ψ^+ and Ψ^- will destabilize their Fermi surface and engender a condensate $\langle\Psi^+\Psi^-\rangle \neq 0$ that breaks $\mathrm{U}(1)_B$ symmetry spontaneously. [Note that $\Psi^+\Psi^-$ is charge neutral and does not break U(1) gauge symmetry.]

In Phase III the long-distance theory comprises a massless photon and neutral fermions $\Psi^{\mathsf{A}=3}$ at finite μ. It naively appears as though $\mathrm{U}(1)_B$ symmetry is unbroken, but as will be shown in Sec. III C, it could be spontaneously broken through an effective interaction mediated by heavy charged particles. Recalling the intuitive pictures for Phases

[7]Notice that the scale of μ is extremely high in this dimensionally reduced theory: $\mu/g_3^2 = \hat{\mu}/g^2 \sim 1/g^2 \gg 1$.

[8]This situation is analogous to center-stabilized QCD with fundamental fermions in $\mathbb{R}^3 \times S^1$ [16,58].

I and II above, we conjecture that actually $\mathrm{U}(1)_B$ is broken *everywhere* in the phase diagram (Fig. 6).[9]

B. Monopoles, bions, and semiclassical confinement

Let us focus on Phase III for $N_c = 2$ and $N_f^{\mathrm{D}} = 1$. We assume $m = 0$ for simplicity and switch to the two-component notation $\Psi^{\mathsf{A}=3} = L^{-1/2}\begin{pmatrix}\psi_1\\ \sigma^2\psi_2^*\end{pmatrix}$, thereby ensuring that $\psi_{1,2}$ possess the canonical dimension of spinors in three dimensions. The tree-level effective theory at small L reads

$$S = \int \mathrm{d}^3x \left[\frac{1}{4g_3^2}F_{ij}^2 + \psi_1^\dagger(i\sigma^i\partial_i - \mu)\psi_1 + \psi_2^\dagger(i\sigma^i\partial_i + \mu)\psi_2\right], \tag{23}$$

where $\sigma^{1,2,4} \equiv (\sigma^1, \sigma^2, -i\mathbb{1}_2)$ and g_3 is defined in (22). Notice that $\mu \neq 0$ breaks the global $\mathrm{SU}(2)_f$ symmetry down to $\mathrm{U}(1)_B$ that rotates $\psi_1 \to e^{i\varphi}\psi_1$ and $\psi_2 \to e^{-i\varphi}\psi_2$.

At a nonperturbative level, we also have instanton-monopoles, reflecting the compact nature of the U(1) gauge group. At first sight, Polyakov's mechanism of confinement due to Debye screening by monopoles [60] seems to apply, but this is not the case here: monopoles are accompanied by fermionic zero modes[10] and do not generate a mass gap for photons [62].[11,12] The effective theory at length scales $\gg L/g$ gains an additional piece that accounts for this effect [15,17]:

$$\delta S = G\int \mathrm{d}^3x[\cos\chi \cdot \det_{1\le I,J\le 2N_f^{\mathrm{D}}}(\psi_I^{\mathrm{T}}\sigma^2\psi_J) + \mathrm{H.c.}], \tag{24}$$

where the scalar field $\chi(x)$ is a dual photon with 2π-periodicity, related to the original field via the Abelian duality relation as $F_{ij} \sim \varepsilon_{ijk}\partial_k\chi$. The monopole operator ('t Hooft–type vertex for the monopole) (24) evidently respects the $\mathrm{SU}(2)_f$ flavor symmetry. One can also check that (24) is invariant under the anomaly-free discrete subgroup $(\mathbb{Z}_8)_A$, which acts as $\psi \to e^{i2\pi/8}\psi$, and $\chi \to \chi + \pi$. The factor G can be extracted from the monopole measure; see Sec. 4 of Ref. [17].[13] Up to an $\mathcal{O}(1)$ numerical factor,

$$\begin{aligned} G &\sim g^{-4}e^{-4\pi^2/g^2}L^{4N_f^{\mathrm{D}}-3} \\ &= g^{-4}e^{-4\pi^2/g^2}L \quad \text{for } N_f^{\mathrm{D}} = 1, \end{aligned} \tag{25}$$

where $g = g(L^{-1})$ is the renormalized coupling at the scale L^{-1}.

1. Magnetic bion formation at $\mu \neq 0$

In order to see mass gap generation for photons, one needs to go to the next order in the semiclassical expansion. The point is that due to the compactness of the A_3 holonomy there is an additional class of monopole-instanton (called KK monopoles) in $\mathbb{R}^3 \times S^1$ [12–14].

There exists a topologically neutral, but magnetically charged combination of the BPS-monopole with a KK-antimonopole called the "magnetic bion" [15], which induces the operator $(\cos 2\chi)$. Note that this operator is invariant under the action of discrete chiral symmetry $\chi \to \chi + \pi$. In some respect, this phenomenon is similar to the formation of instanton–anti-instanton molecules in thermal QCD [65,66], and in others it differs from it as the magnetic bion still has a topological quantum number for its magnetic charge. The physics of multi-instanton correlation in QCD with chemical potential has been studied in, e.g., Refs. [8,9,11]. In quark matter at high density, instantons of large sizes are exponentially suppressed due to the Debye screening of color-electric fields inside instantons [5]. In contrast, this is of no concern here because the medium of $\Psi^{\mathsf{A}=3}$ is transparent for monopoles.

Below, we would like to explicitly calculate the effect of chemical potential μ on the magnetic bion formation. The operator $\mathcal{B}(x)$ of a magnetic bion involves a connected correlator of two monopole operators [15,17],

$$\mathcal{B}(x) \sim G^2 e^{2i\chi(x)}\int \mathrm{d}^3y e^{-V_{\mathrm{C}}(y)}\langle \det(\psi\psi(y))\det(\psi^\dagger\psi^\dagger(0))\rangle, \tag{26}$$

with the repulsive Coulomb potential

$$V_{\mathrm{C}}(y) \equiv \frac{4\pi}{g_3^2}\frac{1}{|y|}. \tag{27}$$

At distances $\gg L$ the correlator of 't Hooft vertices in (26) can be computed with a free fermion propagator $S_{\mathrm{F}}(x;\mu) = \langle\psi_1(x)\psi_1^\dagger(0)\rangle$ and $S_{\mathrm{F}}(x;-\mu) = \langle\psi_2(x)\psi_2^\dagger(0)\rangle$, resulting in

[9] This is a hypothesis at exactly zero temperature. As soon as the imaginary-time direction is compactified, the true symmetry breaking would be replaced with a quasi-long-range order [59].

[10] For the index theorem at finite μ, see Refs. [29,40,61].

[11] The fermionic zero modes of monopoles are absent if one starts from a genuine compact U(1) theory rather than breaking a non-Abelian group with a Higgs mechanism. In such a case the dynamics of monopoles at long distances can be different from that in $\mathbb{R}^3 \times S^1$; see, e.g., Refs. [63].

[12] When $m \neq 0$, fermionic zero modes can be soaked up by the mass term and monopoles are allowed to yield a bosonic potential [49,64]. Similarly, if the difermion condensate $\langle\psi\psi\rangle$ forms dynamically, it would lift the fermionic zero modes and induce a potential. As we will see in Sec. III C, indeed such a condensate can form, but it occurs only at a supersoft scale and can be safely ignored at the scale of average monopole-monopole separation $\sim L\exp(S_m/3)$.

[13] Normalization of the fermion kinetic term in (23) is different from that in Ref. [17].

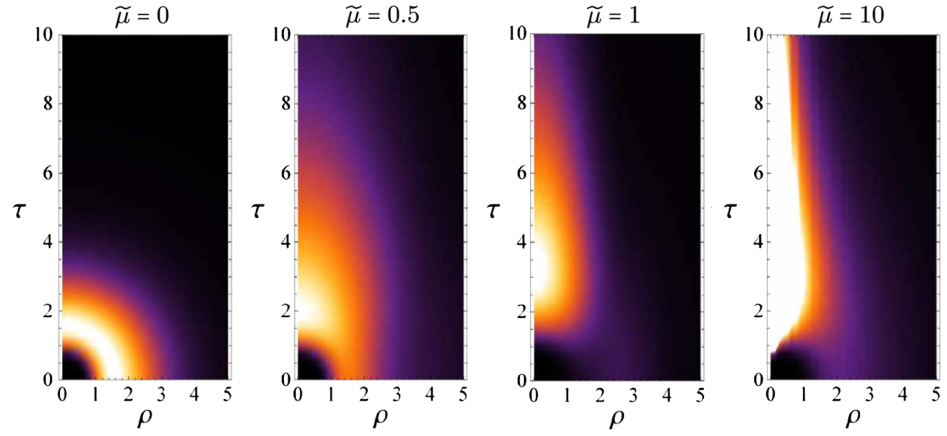

FIG. 10. The probability density $w(\rho, \tau; \tilde{\mu})$ of a magnetic bion (37). Brighter regions have larger w.

$$\begin{aligned}&\langle \det(\psi\psi(x))\det(\psi^\dagger\psi^\dagger(0))\rangle \\ &\quad\propto \mathrm{tr}[S_F(x;\mu)S_F^\dagger(x;\mu)]\mathrm{tr}[S_F(x;-\mu)S_F^\dagger(x;-\mu)] \\ &\quad\propto \{(\partial_1 D_+)^2+(\partial_2 D_+)^2+[(\partial_4-\mu)D_+]^2\} \\ &\qquad\times\{(\partial_1 D_-)^2+(\partial_2 D_-)^2+[(\partial_4+\mu)D_-]^2\},\end{aligned} \tag{28}$$

where $D_\pm(x) \equiv D(x;\pm\mu)$ is a bosonic propagator that solves the Klein-Gordon-type equation

$$[-\partial_1^2-\partial_2^2-(\partial_4-\mu)^2]D(x;\mu)=\delta(x). \tag{29}$$

The explicit form of $D(x;\mu)$ and its properties are summarized in Appendix B. In the above we used (B3) there. At $\mu = 0$, $D \propto |x|^{-1}$ and the correlator (28) is just proportional to $|x|^{-8}$. However, once $\mu \neq 0$, there is anisotropy in space ($x^{1,2}$) and imaginary time (x^4); the weight (28) exhibits a Friedel-type oscillation in spatial directions, reflecting the presence of a sharp Fermi surface, which tends to render bions anisotropic.

Recalling that the three-dimensional Coulomb interaction is governed by the dimensionful coupling $g_3^2 \equiv g^2/L$, it naturally follows that the strength of the bion deformation is measured by the ratio

$$\tilde{\mu} \equiv \frac{\mu}{g_3^2} = \frac{\mu L}{g^2}. \tag{30}$$

If we fix μ and let $L \to 0$, then $\tilde{\mu} \sim \mu L \log\frac{1}{L\Lambda} \to 0$; i.e., the effect of μ on bions inevitably disappears. In order to see a nontrivial deformation of bions one has to increase μ in the course of compactification so that $\mu \gtrsim \frac{1}{L\log\frac{1}{L\Lambda}}$. At the same time, the condition $\mu < \frac{1.98}{L}$ must also be satisfied, in order to stay inside Phase III (cf. Fig. 2).

To simplify the $\tilde{\mu}$ dependence of the weight we make all variables dimensionless in units of g_3^2:

$$\tilde{y} \equiv g_3^2 y, \tag{31}$$

$$\rho \equiv \sqrt{\tilde{y}_1^2+\tilde{y}_2^2}, \tag{32}$$

$$\tau \equiv \tilde{y}_4, \tag{33}$$

$$\tilde{D}_\pm(\rho,\tau) \equiv g_3^{-2} D(y;\pm\mu). \tag{34}$$

Using (25) we find that the bion amplitude is given by

$$\mathcal{B}(x) \sim L^{-3} g^2 e^{-8\pi^2/g^2} W(\tilde{\mu}) e^{2i\chi(x)} \tag{35}$$

with a dimensionless function W defined by

$$W(\tilde{\mu}) \equiv \int_0^\infty \mathrm{d}\rho\rho \int_{-\infty}^\infty \mathrm{d}\tau w(\rho,\tau;\tilde{\mu}), \tag{36}$$

$$\begin{aligned}w(\rho,\tau;\tilde{\mu}) \equiv{}& e^{-4\pi/\sqrt{\rho^2+\tau^2}}\{(\partial_\rho \tilde{D}_+)^2+[(\partial_\tau-\tilde{\mu})\tilde{D}_+]^2\} \\ &\times\{(\partial_\rho \tilde{D}_-)^2+[(\partial_\tau+\tilde{\mu})\tilde{D}_-]^2\}.\end{aligned} \tag{37}$$

The prefactors in (35) are in precise agreement with Refs. [17,67] for the case of two Weyl fermions.

All the $\tilde{\mu}$ dependence is now encapsulated in w. As displayed in Fig. 10, w dramatically changes its profile as a function of $\tilde{\mu}$. At $\tilde{\mu} = 0$, w is isotropic with a sharp peak along the circle $\sqrt{\rho^2+\tau^2} = \pi/2 \simeq 1.57$. This implies that the typical size of a magnetic bion is $\pi/(2g_3^2) = \pi L/(2g^2)$, as noted in Refs. [17,67]. As $\tilde{\mu}$ grows, the weight of w gradually moves to higher τ, with a peak position at $\tau \sim 3$. At $\tilde{\mu} = 10$, w is further focused on the τ axis with a quite narrow range of $\rho \ll 1$. This means that the magnetic bion tends to be rigidly oriented in the x^4 direction. One can also see a ripplelike pattern in the rightmost plot of Fig. 10, caused by a Friedel oscillation of $\tilde{D}$.

Our numerical analysis indicates that the global maximum of w is always located on the τ axis, so let us examine the behavior of w at $\rho = 0$ more closely. Using $\partial_\rho \tilde{D} \to 0$ as

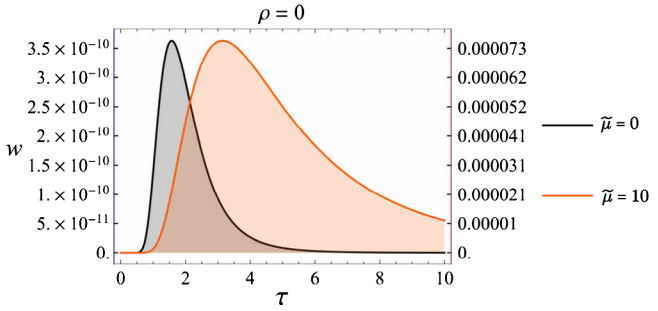

FIG. 11. Comparison of w at $\rho = 0$, (38), for $\tilde{\mu} = 0$ and $\tilde{\mu} = 10$. The scale on the left (right) vertical axis applies to $\tilde{\mu} = 0$ ($\tilde{\mu} = 10$), respectively.

$\rho \to 0$, one gets $w(0,\tau;\tilde{\mu}) = e^{-4\pi/\tau}[(\partial_\tau - \tilde{\mu})\tilde{D}_+]^2[(\partial_\tau + \tilde{\mu})\tilde{D}_-]^2$. Substituting the analytic form (B7) of $\tilde{D}$ in Appendix B one obtains

$$w(0,\tau;\tilde{\mu}) = \frac{e^{-4\pi/\tau}}{(4\pi)^4}\frac{(1+\tilde{\mu}\tau)^2(-1+\tilde{\mu}\tau+2e^{-\tilde{\mu}\tau})^2}{\tau^8} \tag{38}$$

for $\tau > 0$. It shows that the peak of w evolves from $\tau = \pi/2$ at $\tilde{\mu} = 0$ to $\tau = \pi$ at $\tilde{\mu} \gg 1$. This behavior is illustrated in Fig. 11.

In summary, we have found two features of magnetic bions at $\mu \gtrsim \frac{1}{L\log\frac{1}{L\Lambda}}$. First, the monopole-antimonopole pair inside a bion is predominantly oriented in the imaginary-time direction. This is due to the fact that fermions with μ favor hopping in the temporal direction, which has been observed in the context of instantons in dense matter as well [9,11]. Secondly, the bion has a typical size $\pi/g_3^2 = \pi L/g^2$. This is twice as large as that at $\mu = 0$.

2. Semiclassical confinement at $\mu \neq 0$

If we replace the integral of w with its peak value, we obtain a crude estimate:

$$W(\tilde{\mu}) \propto \tilde{\mu}^4 \quad \text{at } \tilde{\mu} \gg 1. \tag{39}$$

It has an interesting implication for the dual photon mass. Let us recall that in addition to (35) there are also operators associated with antibions. Their sum reads

$$\mathcal{B} + \mathcal{B}^\dagger \sim L^{-3}g^2 e^{-8\pi^2/g^2} W(\tilde{\mu})\cos(2\chi). \tag{40}$$

This potential has minima at $\chi = 0$ and π associated with the spontaneous breaking of discrete chiral symmetry. (Note that an order parameter for the discrete chiral symmetry is $e^{i\chi}$ and the two vacua correspond to $\langle e^{i\chi}\rangle = \pm 1$.) At these points the dual photon χ acquires a nonperturbative mass gap, given by

$$M_\chi \sim \frac{1}{L} e^{-4\pi^2/g^2}\sqrt{W(\tilde{\mu})}. \tag{41}$$

This means that the perturbatively massless photon is Debye-screened by the plasma of magnetic bions [15]. The fact that $W(\tilde{\mu})$ asymptotically increases with $\tilde{\mu}$ implies that μ tends to *enhance* the nonperturbative effect on the gauge field.

Using (39) and the one-loop β function for g,

$$e^{-4\pi^2/g^2} \sim (L\Lambda)^{7/3}, \tag{42}$$

one finds

$$\frac{M_\chi}{\Lambda} \sim (L\Lambda)^{4/3}\tilde{\mu}^2 \sim \left(\log\frac{1}{L\Lambda}\right)^2 (L\Lambda)^{10/3}\left(\frac{\mu}{\Lambda}\right)^2, \tag{43}$$

with a renormalization-group invariant scale Λ. The mass gap for the dual photon implies that the fundamental Wilson loop in $\mathbb{R}^3$ obeys area law; quarks are permanently confined. The string tension is given by $T \sim \frac{g^2}{L} M_\chi$ [60]. The L dependence follows from (42) and (43) as

$$\frac{T}{\Lambda^2} \sim \left(\log\frac{1}{L\Lambda}\right)(L\Lambda)^{7/3}\left(\frac{\mu}{\Lambda}\right)^2. \tag{44}$$

This estimate is valid for μ in the range

$$\frac{1}{L\log\frac{1}{L\Lambda}} \ll \mu < \frac{1.98}{L}. \tag{45}$$

C. Superfluidity

Generically a fermionic system at finite density can be unstable toward pair condensation if there is an attractive channel in their interaction. It is therefore important to ask what interactions can happen for $\psi_{1,2}$ in the effective theory (23). Although they do not couple to photons by themselves, they interact through *two* mechanisms of different physical origins. The first one is mediated by monopole-instantons. As was shown in the previous section, the dual photons are screened at distances beyond $1/M_\chi$. As χ settles in one of the two minima $\{0,\pi\}$ of the potential (40),[14] one obtains from (24) a four-fermion operator:

$$\pm G[\det_{I,J}(\psi_I^{\mathrm{T}}\sigma^2\psi_J) + \text{H.c.}]. \tag{46}$$

Note that the 4d instanton would induce an eight-fermion operator, with much weaker coefficient (of order G^2). In this sense, the monopole-instantons are much more important than 4d instantons.

Yet another kind of interaction stems from integrating out heavy $\Psi^\pm$ and $W^\pm$ that are charged under U(1). As an

[14]This breaks the anomaly-free axial $\mathbb{Z}_8$ down to $\mathbb{Z}_4$ spontaneously.

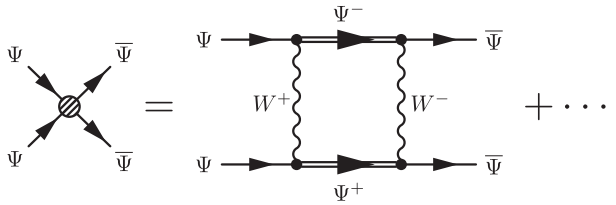

FIG. 12. A four-fermion operator that arises from integrating out heavy charged particles.

example, we show in Fig. 12 an effective interaction in the diquark channel where the four-component Dirac spinor in the Cartan subalgebra $\Psi^{A=3}$ is notated by Ψ. There are a myriad of operators that can be perturbatively generated this way, e.g., $(\overline{\Psi}\gamma^3\Psi)^2$, $(\overline{\Psi}\gamma^i\Psi)^2$, and $(\overline{\Psi}\gamma^3\gamma^i\gamma^j\Psi)^2$, to name but a few. They are all invariant under $\mathrm{U}(1)_A$ and hence do not couple to the dual photon. Here we do not systematically enumerate all possible forms of the interaction, but instead try to capture an essential physical outcome by considering the minimal interaction in the (pseudo)scalar channel,

$$-H[(\overline{\Psi}\Psi)^2+(\overline{\Psi}i\gamma_5\Psi)^2+|\Psi^{\mathrm{T}}C\Psi|^2+|\Psi^{\mathrm{T}}C\gamma_5\Psi|^2], \quad (47)$$

with a charge-conjugation matrix $C=\mathrm{diag}(-\sigma^2,\sigma^2)$ and $\gamma_5=\mathrm{diag}(\mathbb{1}_2,-\mathbb{1}_2)$. This interaction, being perturbatively induced, preserves $\mathrm{U}(1)_A\times\mathrm{SU}(2)_f$ [68]. The coupling H should be $\propto L$ according to dimensional analysis, and it must be multiplied by g^4 because there are at least four bare vertices in the process of Fig. 12. Thus

$$H\propto g^4L. \quad (48)$$

Since G [cf. (25)] is proportional to $e^{-4\pi^2/g^2}\ll 1$, (48) means that $|H|\gg G$.

The sign of H is not fixed by symmetries alone. In this regard we would like to note that the process of Fig. 12 is of the same kind as the van der Waals interaction in QED, which originates from the two-photon exchange and is attractive because it arises at second order in perturbation theory [69]. A similar long-range force between color-singlet hadrons in QCD, originating from the two-gluon exchange process, is also known to be attractive [70–72]. Therefore in the following analysis we will assume $H>0$ and pursue its physical consequences, leaving a microscopic verification to future work. We remark that the phase diagram shown earlier as Fig. 1 was also based on the assumption that $H>0$.

1. Fermionic effective theory

Incorporating both types of interactions [(46) and (47)] and dropping the quark-antiquark vertices because they are not relevant to the BCS instability, we end up with the fermionic effective theory

$$S=\int \mathrm{d}^3x\{\overline{\Psi}(\gamma_i\partial_i-\mu\gamma_4)\Psi\pm G[\det_{I,J}(\psi_I^{\mathrm{T}}\sigma^2\psi_J)+\mathrm{H.c.}] - H(|\Psi^{\mathrm{T}}C\Psi|^2+|\Psi^{\mathrm{T}}C\gamma_5\Psi|^2)\}, \quad (49)$$

where the sign in front of G depends on whether $\langle\chi\rangle=0$ or π. Analogous four-fermion models in three and four dimensions have been studied before [73,74]. We note that while the models in Refs. [73,74] were introduced on phenomenological grounds, (49) is a faithful description of the microscopic dynamics of adjoint QCD in the circle-compactification limit.

A remark on the parity of the ground state is in order. Because the second line of (49) does *not* distinguish between 0^+ and 0^- diquarks, one shall look at the monopole-induced operator. With the help of the relation

$$\det_{I,J}(\psi_I^{\mathrm{T}}\sigma^2\psi_J)+\mathrm{H.c.}=\frac{3}{2}[(\psi_1^{\mathrm{T}}\sigma^2\psi_1)(\psi_2^{\mathrm{T}}\sigma^2\psi_2)+\mathrm{H.c.}] =\frac{3}{4}(|\Psi^{\mathrm{T}}C\Psi|^2-|\Psi^{\mathrm{T}}C\gamma_5\Psi|^2), \quad (50)$$

we observe that interaction in the 0^+ channel is stronger than 0^- for $\langle\chi\rangle=0$. However the opposite happens in the other vacuum $\langle\chi\rangle=\pi$. Thus, after all, the effective theory (49) *per se* does not uniquely determine the parity of the ground state and prompts us to add a small but nonzero external source field to resolve the ambiguity. If one inserts to the action a real mass term $m\overline{\Psi}\Psi$ with an arbitrarily small m, the ambiguity is resolved.[15] There are two ways to check this. First, one can invoke QCD inequalities generalized to $\mu\neq 0$ [40,75,77] to argue that $\Psi^{\mathrm{T}}C\gamma_5\Psi$ is the lightest bilinear field.[16] We stress that this argument works equally in both $\mathbb{R}^4$ and $\mathbb{R}^3\times S^1$. The second argument to check parity only works in the semiclassical small-L regime. Namely, when the above sources are present in the action, they will absorb the fermionic zero modes inhabiting the monopoles and allow for a bosonic potential $\sim m^2\cos\chi$ to be generated on top of the bion-induced potential (40). This potential, however small in magnitude, can and does lift the degeneracy between $\chi=0$ and π, and consequently fixes the parity of the ground state.

From the consideration above, one may assume that the interaction is stronger for the 0^+ channel than for 0^-, tacitly assuming the presence of a suitable infinitesimal external field in the action. Now, since the monopole-induced interaction is nonperturbatively small, it can be safely dropped, and we arrive at a simpler theory that sufficiently

[15] In QCD-like theories at finite density [33,75,76], the parity of the diquark or pion condensate was automatically determined because the parity of the ground state at zero chemical potential was fixed by a real mass term.

[16] This observation lends support to our strategy to consider a simplified effective theory (47) from the very beginning.

serves our purpose of probing the ground state of the fermionic sector:

$$S = \int \mathrm{d}^3x[\overline{\Psi}(\gamma_i\partial_i - \mu\gamma_4)\Psi - H|\Psi^{\mathrm{T}}C\gamma_5\Psi|^2]. \quad (51)$$

2. Gap equation

We solve the theory in the mean-field approximation following the standard procedure [46,78]. This is expected to be accurate, given the smallness of the coupling $H\mu \propto g^4\hat{\mu} \ll 1$. The Hubbard-Stratonovich transformation applied to (51) with an auxiliary complex field $\Delta(x)$ yields

$$S = \int \mathrm{d}^3x\left[\overline{\Psi}(\gamma_i\partial_i - \mu\gamma_4)\Psi + \frac{|\Delta|^2}{4H} - \frac{1}{2}(\Delta^*\Psi^{\mathrm{T}}C\gamma_5\Psi + \mathrm{H.c.})\right]. \quad (52)$$

With a suitable $\mathrm{U}(1)_B$ rotation, one can take $\Delta \geq 0$ without loss of generality. In the Nambu-Gor'kov basis $(\Psi, C\overline{\Psi}^{\mathrm{T}})$ we have for the energy density

$$\begin{aligned} U(\Delta) &\equiv -\frac{1}{V_{\mathbb{R}^3}}\log Z \\ &= \frac{\Delta^2}{4H} - \frac{1}{2}\int\frac{\mathrm{d}^3p}{(2\pi)^3}\mathrm{tr}\log\begin{pmatrix}\Delta\gamma_5 & i\not{p}+\mu\gamma_4\\ i\not{p}-\mu\gamma_4 & -\Delta\gamma_5\end{pmatrix} \\ &= \frac{\Delta^2}{4H} - \int\frac{\mathrm{d}^3p}{(2\pi)^3}\{\log[p_4^2 + (|\boldsymbol{p}_\perp| - \mu)^2 + \Delta^2] \\ &\quad + \log[p_4^2 + (|\boldsymbol{p}_\perp| + \mu)^2 + \Delta^2]\} \\ &= \frac{\Delta^2}{4H} - \int'\frac{\mathrm{d}p_1\mathrm{d}p_2}{(2\pi)^2}\left\{\sqrt{(|\boldsymbol{p}_\perp| - \mu)^2 + \Delta^2}\right. \\ &\quad \left. + \sqrt{(|\boldsymbol{p}_\perp| + \mu)^2 + \Delta^2}\right\}. \end{aligned} \quad (53)$$

The final integral with a prime is to be regularized with a cutoff. Then the gap equation $\partial U(\Delta)/\partial\Delta = 0$ for a nontrivial solution $\Delta \neq 0$ is given by

$$\frac{1}{H} = \int'\frac{\mathrm{d}p\,p}{\pi}\left(\frac{1}{\sqrt{(p-\mu)^2+\Delta^2}} + \frac{1}{\sqrt{(p+\mu)^2+\Delta^2}}\right). \quad (54)$$

As $\Delta \to 0$ the first term yields IR divergence at the Fermi surface. Retaining only the first term and imposing a momentum cutoff $\Lambda'(> \mu)$, one obtains

$$\frac{1}{H} \simeq \frac{\mu}{\pi}\log\frac{4\mu(\Lambda'-\mu)}{\Delta^2}, \quad (55)$$

or

$$\Delta \propto \sqrt{\mu(\Lambda'-\mu)}\exp\left(-\frac{\pi}{2H\mu}\right). \quad (56)$$

Physically, this means that fermions acquire an energy gap Δ and the $\mathrm{U}(1)_B$ symmetry is spontaneously broken by the condensate $\langle\Psi^{\mathrm{T}}C\gamma_5\Psi\rangle \neq 0$; the system is in a superfluid phase.[17] We stress that the parity of the diquark condensate is the same at small L and large L [recall our remarks below (50)]. Note that in this analysis the density of fermions need not be high; the computation in this section is valid for any $\mu > 0$ as long as we are in Phase III ($\mu < 1.98/L$), which means that superfluidity may take place at *arbitrarily small* μ. This is a remarkable result.

Plugging (48) and $\Lambda' \sim L^{-1}$ into (56), we gain the crude estimate

$$\Delta \propto \frac{\sqrt{\hat{\mu}}}{L}\exp\left(-\frac{1}{g^4\hat{\mu}}\right). \quad (57)$$

Notably, this ultrasoft scale is far smaller than the dual photon mass $M_\chi \propto L^{-1}\exp(-4\pi^2/g^2)$ and is invisible at any finite order of the semiclassical expansion. Since the extent of the Cooper pair $1/\Delta$ far exceeds the typical bion size, the diquark condensate is not expected to modify the fermion-binding mechanism of bions in Sec. III B.

The various length scales in Phase III may be summarized as follows:

$$\begin{array}{ccccccccccc} r_{\mathrm{m}} & \lesssim & d_{\psi-\psi} & \ll & r_{\mathrm{b}} & \ll & d_{\mathrm{m-m}} & \ll & d_{\mathrm{b-b}} & \ll & \frac{1}{M_\chi} \\ \downarrow & & \downarrow & & \downarrow & & \downarrow & & \downarrow & & \downarrow \\ L & & \frac{1}{\mu} & & \frac{L}{g^2} & & Le^{S_{\mathrm{m}}/3} & & Le^{2S_{\mathrm{m}}/3} & & Le^{S_{\mathrm{m}}} \end{array} \quad \begin{array}{c} \ll \quad \frac{1}{\Delta} \\ \downarrow \\ \frac{L}{\sqrt{\hat{\mu}}}\exp\left(\frac{1}{g^4\hat{\mu}}\right), \end{array} \quad (58)$$

where r_{m} is the monopole size, $d_{\psi-\psi}$ is the interquark distance, r_{b} is the bion size, $d_{\mathrm{m-m}}$ is the intermonopole distance, $d_{\mathrm{b-b}}$ is the interbion distance, $1/M_\chi$ is the inverse Debye screening length, $1/\Delta$ is the Cooper-pair size, and $S_{\mathrm{m}} = 4\pi^2/g^2$ is the monopole action.

[17] Since Ψ does not couple to the U(1) photon, this phase is not a superconductor.

3. Low-energy effective theory for superfluid phonons

In the far-infrared limit at energies below Δ, the effective degree of freedom is phonon, i.e., the Nambu-Goldstone mode associated with the baryon number. It emerges as a phase fluctuation of the condensate and can be introduced as $\Delta \to \Delta e^{2i\phi(x)}$. The low-energy effective theory of phonons can be derived by expanding the functional determinant of Ψ in powers of the derivative of ϕ (the so-called gradient expansion [79]). The result is

$$\mathcal{L}_{\rm eff} = f^2[(\partial_4\phi)^2 + v^2\{(\partial_1\phi)^2 + (\partial_2\phi)^2\}], \quad (59)$$

with

$$f^2 = \frac{\mu}{2\pi}, \qquad v^2 = \frac{1}{2}. \quad (60)$$

The factor of 2 in the denominator of v^2 reflects the dimensionality of space. The effective theory (59) can also be derived from the equation of state $P = \mu^3/(6\pi)$ on the basis of symmetry arguments along the lines of Ref. [80]. Equation (60) should be contrasted with $f^2 \sim \mu^2$ and $v^2 = 1/3$ for the Nambu-Goldstone modes in high-density quark matter in four dimensions [81–83].

IV. CONCLUSION

In this paper we extended the bion mechanism of confinement [15] to nonzero quark chemical potential μ in adjoint QCD with *spatial* compactification. In the first part, we performed a perturbative analysis of the Wilson line potential (whose result gives a realization of the Hosotani mechanism) in the presence of μ and revealed a rich phase diagram in the space of μ and m. In the second part we studied the μ dependence of semiclassical configurations (monopoles and their molecules called magnetic bions) in the center-symmetric phase. In addition to the Coulomb interaction, monopole-instantons also talk to each other via a fermion zero mode exchange, which at $\mu \neq 0$ is modified due to the anisotropic hopping amplitude of fermions. Consequently, bions favor a temporal orientation and their amplitude grows with μ, leading to a larger mass gap of photons and a greater string tension. Intriguingly, neutral massless fermions that are free in the leading-order perturbation theory may exhibit novel superfluidity triggered by the combination of perturbatively induced four-fermion operators and nonperturbatively induced monopole operators ('t Hooft vertex). The analysis in this paper remains valid at any $\mu \neq 0$ as long as the compactified direction S^1 is small enough. It would be interesting to examine the dimensional crossover from small to large S^1 (Fig. 1) in future lattice simulations, to clarify how the BEC-BCS crossover region in $\mathbb{R}^4$ is connected to the exotic phase structure in $\mathbb{R}^3 \times S^1$ found in this work. Dimensional crossover of an interacting Fermi gas has been actively investigated in the condensed matter physics community [84] and it is of great interest to see what new physics will emerge for the case of relativistic quark matter.

ACKNOWLEDGMENTS

We are grateful to A. Cherman and T. Sulejmanpasic for valuable comments on the manuscript. T. K. was supported by the RIKEN Interdisciplinary Theoretical Science Research Group (iTHES) project. N. Y. was supported by The Japan Society for the Promotion of Science (JSPS) KAKENHI Grant No. 16K17703 and the Ministry of Education, Culture, Sports, Science and Technology of Japan (MEXT)-Supported Program for the Strategic Research Foundation at Private Universities, "Topological Science" (Grant No. S1511006). M. Ü. was supported by the Department of Energy (DOE) under Grant No. DE-SC0013036.

APPENDIX A: ONE-LOOP EFFECTIVE POTENTIAL

Below we will outline the derivation of the formula (17). Let us momentarily put the system in a box of linear extent $L_\perp \times L_\perp \times L \times \beta$, with β the inverse temperature and $L_\perp$ the length in the $x^{1,2}$ directions. The Euclidean Dirac operator in the background (9) reads

$$\not{D}(\mu) = \gamma_1\partial_1 + \gamma_2\partial_2 + \gamma_3 D_3^{\rm ad} + \gamma_4(\partial_4 - \mu), \quad (A1)$$

where $D_3^{\rm ad}$ is the adjoint covariant derivative that acts on a matrix test field $v = (v_{\rm ab})$ as

$$(D_3^{\rm ad} v)_{\rm ab} \equiv (\partial_3 v + i[A_3, v])_{\rm ab} \quad (A2)$$

$$= [\partial_3 + i(a_{\rm a} - a_{\rm b})]v_{\rm ab}. \quad (A3)$$

Since each component of v except for its trace can be regarded as independent, we get [1]

$$\begin{aligned}
\Gamma_q(\Omega;\mu) &= \frac{1}{2}\mathrm{tr}\log[-\not{D}(\mu)^2 + m^2] \\
&= 2\mathrm{tr}\log[-\partial_1^2 - \partial_2^2 - (D_3^{\rm ad})^2 - (\partial_4 - \mu)^2 + m^2] \\
&= 2L_\perp^2 \int \frac{dp_1 dp_2}{(2\pi)^2} \sum_{p_3}\sum_{p_4}\left(\sum_{\rm a,b=1}^{N_c} \log[p_\perp^2 + (p_3 + a_{\rm a} - a_{\rm b})^2 + (p_4 + i\mu)^2 + m^2] - \log[\boldsymbol{p}^2 + (p_4 + i\mu)^2 + m^2]\right) \\
&= L_\perp^2 \int \frac{dp_1 dp_2}{(2\pi)^2} \sum_{p_3}\sum_{p_4}\left\{\sum_{\rm a,b=1}^{N_c} (\log[p_4^2 + (\mathcal{E}_{\rm ab} + \mu)^2] + \log[p_4^2 + (\mathcal{E}_{\rm ab} - \mu)^2])\right. \\
&\quad \left. - \log[p_4^2 + (\mathcal{E} + \mu)^2] - \log[p_4^2 + (\mathcal{E} - \mu)^2]\right\}, \quad (A4)
\end{aligned}$$

where $p_\perp^2 \equiv p_1^2 + p_2^2$, $\boldsymbol{p}^2 \equiv p_\perp^2 + p_3^2$, $p_3 = \frac{2n\pi}{L}(n \in \mathbb{Z})$, $p_4 = \frac{(2\ell+1)\pi}{\beta}(\ell \in \mathbb{Z})$, $\mathcal{E} \equiv \sqrt{\boldsymbol{p}^2 + m^2}$, and

$$\mathcal{E}_{\mathtt{ab}} \equiv \sqrt{p_\perp^2 + (p_3 + a_{\mathtt{a}} - a_{\mathtt{b}})^2 + m^2}. \tag{A5}$$

The summation over p_4 can be taken with the standard formula [85]

$$\sum_{\ell=-\infty}^{\infty} \log[(2\ell+1)^2\pi^2 + \omega^2] = \omega + 2\log(1 + e^{-\omega}), \tag{A6}$$

where an ω-independent divergence has been subtracted. We thus obtain

$$\begin{aligned}\Gamma_q(\Omega;\mu) = 2\beta L_\perp^2 \int \frac{\mathrm{d}p_1 \mathrm{d}p_2}{(2\pi)^2} \sum_{p_3} \Bigg\{ \sum_{\mathtt{a},\mathtt{b}=1}^{N_c} \left(\mathcal{E}_{\mathtt{ab}} + \frac{1}{\beta}\log[1 + e^{-\beta(\mathcal{E}_{\mathtt{ab}}+\mu)}] + \frac{1}{\beta}\log[1 + e^{-\beta(\mathcal{E}_{\mathtt{ab}}-\mu)}] \right) \\ - \mathcal{E} - \frac{1}{\beta}\log[1 + e^{-\beta(\mathcal{E}+\mu)}] - \frac{1}{\beta}\log[1 + e^{-\beta(\mathcal{E}-\mu)}] \Bigg\}\end{aligned} \tag{A7}$$

and

$$\begin{aligned}\delta V_{\mathrm{F}}(\Omega;\mu) &= -\lim_{\beta\to\infty} \frac{1}{\beta L_\perp^2 L} \{\Gamma_q(\Omega;\mu) - \Gamma_q(\Omega;0)\} \\ &= -\frac{2}{L} \int \frac{\mathrm{d}p_1 \mathrm{d}p_2}{(2\pi)^2} \sum_{p_3} \Bigg\{ \sum_{\mathtt{a},\mathtt{b}=1}^{N_c} (\mu - \mathcal{E}_{\mathtt{ab}})\theta(\mu - \mathcal{E}_{\mathtt{ab}}) - (\mu - \mathcal{E})\theta(\mu - \mathcal{E}) \Bigg\} \quad \text{for } \mu \geq 0.\end{aligned} \tag{A8}$$

The remaining integral may be done with the formula

$$\int \frac{\mathrm{d}p_1 \mathrm{d}p_2}{(2\pi)^2} \left(\mu - \sqrt{p_\perp^2 + X}\right)\theta\left(\mu - \sqrt{p_\perp^2 + X}\right) = \frac{1}{4\pi}\left(\frac{1}{3}\mu^3 - \mu X + \frac{2}{3}X^{3/2}\right)\theta(\mu^2 - X) \quad \text{for } X \geq 0, \tag{A9}$$

with the result

$$\begin{aligned}\delta V_{\mathrm{F}}(\Omega;\mu) = -\frac{1}{2\pi L} \sum_{p_3} \Bigg\{ \sum_{\mathtt{a},\mathtt{b}=1}^{N_c} \left(\frac{1}{3}\mu^3 - \mu X + \frac{2}{3}X^{3/2}\right)\theta(\mu^2 - X)|_{X=(p_3+a_{\mathtt{a}}-a_{\mathtt{b}})^2+m^2} \\ - \left(\frac{1}{3}\mu^3 - \mu Y + \frac{2}{3}Y^{3/2}\right)\theta(\mu^2 - Y)|_{Y=p_3^2+m^2} \Bigg\}.\end{aligned} \tag{A10}$$

Substituting $p_3 = \frac{2n\pi}{L}(n \in \mathbb{Z})$ into this equation, we finally arrive at (17).

APPENDIX B: FREE PROPAGATORS WITH $\mu \neq 0$ IN THREE DIMENSIONS

We solve for the Euclidean propagators in $2+1$ dimensions in the presence of μ. The fermion propagator S_{F} solves the equation

$$(i\sigma^1\partial_1 + i\sigma^2\partial_2 + \partial_4 - \mu)S_{\mathrm{F}}(x;\mu) = \delta(x)\mathbb{1}_2. \tag{B1}$$

The boson propagator solves the Klein-Gordon equation

$$[-\partial_1^2 - \partial_2^2 - (\partial_4 - \mu)^2]D(x;\mu) = \delta(x). \tag{B2}$$

They are related through

$$S_{\mathrm{F}}(x;\mu) = (i\sigma^1\partial_1 + i\sigma^2\partial_2 - \partial_4 + \mu)D(x;\mu). \tag{B3}$$

It is easy to verify that

$$D(\boldsymbol{x}, x_4;\mu) = D(\boldsymbol{x}, -x_4;-\mu), \qquad \boldsymbol{x} = (x_1, x_2). \tag{B4}$$

Thus one can assume $\mu > 0$ without loss of generality. Writing $r \equiv \sqrt{x_1^2 + x_2^2}$, we have

$$D(x;\mu) = \int \frac{d^3p}{(2\pi)^3} \frac{e^{ipx}}{p_1^2 + p_2^2 + (p_4 + i\mu)^2}$$
$$= \int_{-\infty}^{\infty} dp_4 \int_0^{\infty} \frac{dp_\perp p_\perp}{(2\pi)^3} \int_0^{2\pi} d\theta \frac{e^{ip_\perp r\cos\theta + ip_4 x_4}}{p_\perp^2 + (p_4 + i\mu)^2}$$
$$= \int_{-\infty}^{\infty} dp_4 e^{ip_4 x_4} \int_0^{\infty} \frac{dp_\perp p_\perp}{(2\pi)^2} \frac{J_0(p_\perp r)}{p_\perp^2 + (p_4 + i\mu)^2}$$
$$= \frac{1}{(2\pi)^2} \int_{-\infty}^{\infty} dp_4 e^{ip_4 x_4} K_0\left(\sqrt{(p_4 + i\mu)^2} r\right). \quad \text{(B5)}$$

An alternative expression which has no singularity at $r = 0$ can also be obtained by integrating over p_4 first, with the result

$$D(x;\mu) = \frac{e^{\mu x_4}}{4\pi} \left\{ \frac{1}{\sqrt{r^2 + x_4^2}} - \int_0^{\mu} dp_\perp J_0(p_\perp r) e^{-x_4 p_\perp} \right\}. \quad \text{(B6)}$$

These formulas give access to limiting behaviors of D in some cases of interest:

(i) For $\mu = 0$,

$$D(x;0) = \frac{1}{4\pi\sqrt{r^2 + x_4^2}}. \quad \text{(B7)}$$

(ii) For $r = 0$,

$$D(x;\mu) = \frac{1}{4\pi x_4} \{1 - \theta(-x_4) 2e^{-\mu|x_4|}\}$$
$$\approx \frac{1}{4\pi x_4} \quad \text{for } \mu|x_4| \gg 1. \quad \text{(B8)}$$

(iii) For $x_4 = 0$,

$$D(x;\mu) = \frac{1}{4\pi r} \int_{\mu r}^{\infty} dx J_0(x) \quad \text{(B9)}$$
$$\approx \frac{1}{\sqrt{\mu}} \frac{\cos(\mu r + \frac{\pi}{4})}{(2\pi r)^{3/2}} \quad \text{for } \mu r \gg 1. \quad \text{(B10)}$$

(iv) For $\mu r \gg 1$ with any x_4,

$$D(x;\mu) \approx \frac{r\cos(\mu r + \frac{\pi}{4}) + x_4 \sin(\mu r + \frac{\pi}{4})}{(2\pi)^{3/2}(r^2 + x_4^2)\sqrt{\mu r}}. \quad \text{(B11)}$$

[1] D. J. Gross, R. D. Pisarski, and L. G. Yaffe, Rev. Mod. Phys. **53**, 43 (1981).
[2] T. Schafer and E. V. Shuryak, Rev. Mod. Phys. **70**, 323 (1998).
[3] D. Diakonov, Proc. Int. Sch. Phys. "Enrico Fermi" **130**, 397 (1996); Prog. Part. Nucl. Phys. **51**, 173 (2003).
[4] S. Vandoren and P. van Nieuwenhuizen, arXiv:0802.1862.
[5] E. V. Shuryak, Nucl. Phys. **B203**, 140 (1982).
[6] R. Rapp, T. Schafer, E. V. Shuryak, and M. Velkovsky, Phys. Rev. Lett. **81**, 53 (1998).
[7] M. G. Alford, K. Rajagopal, and F. Wilczek, Phys. Lett. B **422**, 247 (1998).
[8] G. W. Carter and D. Diakonov, Phys. Rev. D **60**, 016004 (1999).
[9] R. Rapp, T. Schafer, E. V. Shuryak, and M. Velkovsky, Ann. Phys. (N.Y.) **280**, 35 (2000).
[10] D. T. Son, M. A. Stephanov, and A. R. Zhitnitsky, Phys. Lett. B **510**, 167 (2001).
[11] T. Schafer, Phys. Rev. D **57**, 3950 (1998); **65**, 094033 (2002).
[12] K.-M. Lee and P. Yi, Phys. Rev. D **56**, 3711 (1997).
[13] K.-M. Lee and C.-h. Lu, Phys. Rev. D **58**, 025011 (1998).
[14] T. C. Kraan and P. van Baal, Nucl. Phys. **B533**, 627 (1998); Phys. Lett. B **435**, 389 (1998).
[15] M. Unsal, Phys. Rev. Lett. **100**, 032005 (2008); Phys. Rev. D **80**, 065001 (2009).
[16] M. Shifman and M. Unsal, Phys. Rev. D **78**, 065004 (2008).
[17] P. C. Argyres and M. Unsal, J. High Energy Phys. 08 (2012) 063.
[18] T. M. W. Nye and M. A. Singer, arXiv:math/0009144.
[19] E. Poppitz and M. Unsal, J. High Energy Phys. 03 (2009) 027.
[20] N. M. Davies, T. J. Hollowood, V. V. Khoze, and M. P. Mattis, Nucl. Phys. **B559**, 123 (1999); N. M. Davies, T. J. Hollowood, and V. V. Khoze, J. Math. Phys. (N.Y.) **44**, 3640 (2003).
[21] M. Unsal and L. G. Yaffe, Phys. Rev. D **78**, 065035 (2008).
[22] P. N. Meisinger and M. C. Ogilvie, Phys. Rev. D **81**, 025012 (2010).
[23] M. C. Ogilvie, J. Phys. A **45**, 483001 (2012).
[24] D. Diakonov, N. Gromov, V. Petrov, and S. Slizovskiy, Phys. Rev. D **70**, 036003 (2004).
[25] Y. Hosotani, Phys. Lett. **126B**, 309 (1983); Ann. Phys. (N.Y.) **190**, 233 (1989).
[26] C. Korthals Altes, R. D. Pisarski, and A. Sinkovics, Phys. Rev. D **61**, 056007 (2000).
[27] J. C. Myers and M. C. Ogilvie, J. High Energy Phys. 07 (2009) 095.
[28] S. Hands, T. J. Hollowood, and J. C. Myers, J. High Energy Phys. 07 (2010) 086.
[29] F. Bruckmann, R. Rodl, and T. Sulejmanpasic, Phys. Rev. D **88**, 054501 (2013).

[30] Y. Liu, E. Shuryak, and I. Zahed, Phys. Rev. D **94**, 105011 (2016).
[31] Q. Chen, J. Stajic, S. Tan, and K. Levin, Phys. Rep. **412**, 1 (2005).
[32] *The BCS-BEC Crossover and the Unitary Fermi Gas*, Lecture Notes in Physics Vol. 836, edited by W. Zwerger (Springer-Verlag, Berlin, 2012).
[33] J. B. Kogut, M. A. Stephanov, D. Toublan, J. J. M. Verbaarschot, and A. Zhitnitsky, Nucl. Phys. **B582**, 477 (2000).
[34] S. Hands, I. Montvay, S. Morrison, M. Oevers, L. Scorzato, and J. Skullerud, Eur. Phys. J. C **17**, 285 (2000).
[35] K. Splittorff, D. T. Son, and M. A. Stephanov, Phys. Rev. D **64**, 016003 (2001).
[36] S. Hands, I. Montvay, L. Scorzato, and J. Skullerud, Eur. Phys. J. C **22**, 451 (2001).
[37] Y. Nishida and H. Abuki, Phys. Rev. D **72**, 096004 (2005).
[38] G.-f. Sun, L. He, and P. Zhuang, Phys. Rev. D **75**, 096004 (2007).
[39] L. He, Phys. Rev. D **82**, 096003 (2010).
[40] T. Kanazawa, T. Wettig, and N. Yamamoto, J. High Energy Phys. 12 (2011) 007.
[41] T. Kanazawa, *Dirac Spectra in Dense QCD*, Springer Theses Vol. 124 (Springer, Japan, 2013).
[42] M. E. Peskin, Nucl. Phys. **B175**, 197 (1980).
[43] D. T. Son, Phys. Rev. D **59**, 094019 (1999).
[44] T. Schafer and F. Wilczek, Phys. Rev. D **60**, 114033 (1999).
[45] D. H. Rischke, D. T. Son, and M. A. Stephanov, Phys. Rev. Lett. **87**, 062001 (2001).
[46] M. Buballa, Phys. Rep. **407**, 205 (2005).
[47] G. Cossu and M. D'Elia, J. High Energy Phys. 07 (2009) 048.
[48] G. Cossu, H. Hatanaka, Y. Hosotani, and J.-I. Noaki, Phys. Rev. D **89**, 094509 (2014).
[49] M. Unsal and L. G. Yaffe, J. High Energy Phys. 08 (2010) 030.
[50] P. N. Meisinger and M. C. Ogilvie, Phys. Rev. D **65**, 056013 (2002).
[51] M. M. Anber and M. Ünsal, J. High Energy Phys. 12 (2014) 107.
[52] A. Vshivtsev, M. Vdovichenko, and K. Klimenko, Zh. Eksp. Teor. Fiz. **114**, 418 (1998) [J. Exp. Theor. Phys. **87**, 229 (1998)].
[53] J. C. Myers and M. C. Ogilvie, Phys. Rev. D **77**, 125030 (2008).
[54] T. Misumi and T. Kanazawa, J. High Energy Phys. 06 (2014) 181.
[55] B. Bringoltz, M. Koren, and S. R. Sharpe, Phys. Rev. D **85**, 094504 (2012).
[56] M. G. Alford, A. Kapustin, and F. Wilczek, Phys. Rev. D **59**, 054502 (1999).
[57] H. Leutwyler and A. V. Smilga, Phys. Rev. D **46**, 5607 (1992).
[58] E. Poppitz and T. Sulejmanpasic, J. High Energy Phys. 09 (2013) 128.
[59] N. D. Mermin and H. Wagner, Phys. Rev. Lett. **17**, 1133 (1966); P. C. Hohenberg, Phys. Rev. **158**, 383 (1967); S. R. Coleman, Commun. Math. Phys. **31**, 259 (1973).
[60] A. M. Polyakov, Nucl. Phys. **B120**, 429 (1977).
[61] R. V. Gavai and S. Sharma, Phys. Rev. D **81**, 034501 (2010).
[62] I. Affleck, J. A. Harvey, and E. Witten, Nucl. Phys. **B206**, 413 (1982).
[63] L. B. Ioffe and A. I. Larkin, Phys. Rev. B **39**, 8988 (1989); J. B. Marston, Phys. Rev. Lett. **64**, 1166 (1990); G. Murthy, Phys. Rev. Lett. **67**, 911 (1991); H. Kleinert, F. S. Nogueira, and A. Sudbo, Phys. Rev. Lett. **88**, 232001 (2002); I. F. Herbut and B. H. Seradjeh, Phys. Rev. Lett. **91**, 171601 (2003); I. F. Herbut, B. H. Seradjeh, S. Sachdev, and G. Murthy, Phys. Rev. B **68**, 195110 (2003); M. Hermele, T. Senthil, M. P. A. Fisher, P. A. Lee, N. Nagaosa, and X.-G. Wen, Phys. Rev. B **70**, 214437 (2004).
[64] E. Poppitz, T. Schafer, and M. Unsal, J. High Energy Phys. 10 (2012) 115.
[65] E.-M. Ilgenfritz and E. V. Shuryak, Phys. Lett. B **325**, 263 (1994).
[66] T. Schafer, E. V. Shuryak, and J. J. M. Verbaarschot, Phys. Rev. D **51**, 1267 (1995).
[67] M. M. Anber and E. Poppitz, J. High Energy Phys. 06 (2011) 136.
[68] T. Zhang, T. Brauner, and D. H. Rischke, J. High Energy Phys. 06 (2010) 064.
[69] L. D. Landau and E. M. Lifshits, *Quantum Mechanics*, Course of Theoretical Physics Vol. 3 (Butterworth-Heinemann, Oxford, 1991).
[70] P. M. Fishbane and M. T. Grisaru, Phys. Lett. B **74B**, 98 (1978).
[71] T. Appelquist and W. Fischler, Phys. Lett. **77B**, 405 (1978).
[72] H. Fujii and D. Kharzeev, Phys. Rev. D **60**, 114039 (1999).
[73] Y. Nambu and G. Jona-Lasinio, Phys. Rev. **122**, 345 (1961); **124**, 246 (1961).
[74] B. Rosenstein, B. J. Warr, and S. H. Park, Phys. Rev. D **39**, 3088 (1989); Phys. Rep. **205**, 59 (1991).
[75] J. B. Kogut, M. A. Stephanov, and D. Toublan, Phys. Lett. B **464**, 183 (1999).
[76] D. T. Son and M. A. Stephanov, Phys. Rev. Lett. **86**, 592 (2001).
[77] A. Cherman and B. C. Tiburzi, J. High Energy Phys. 06 (2011) 034.
[78] T. Hatsuda and T. Kunihiro, Phys. Rep. **247**, 221 (1994).
[79] T. Eguchi, Phys. Rev. D **14**, 2755 (1976).
[80] D. T. Son, arXiv:hep-ph/0204199.
[81] D. T. Son and M. A. Stephanov, Phys. Rev. D **61**, 074012 (2000); **62**, 059902 (2000).
[82] S. R. Beane, P. F. Bedaque, and M. J. Savage, Phys. Lett. B **483**, 131 (2000).
[83] K. Fukushima and K. Iida, Phys. Rev. D **71**, 074011 (2005).
[84] T. Valla, P. D. Johnson, Z. Yusof, B. Wells, Q. Li, S. M. Loureiro, R. J. Cava, M. Mikami, Y. Mori, M. Yoshimura, and T. Sasaki, Nature (London) **417**, 627 (2002); D. S. Petrov, M. A. Baranov, and G. V. Shlyapnikov, Phys. Rev. A **67**, 031601 (2003); P. Dyke, E. D. Kuhnle, S. Whitlock, H. Hu, M. Mark, S. Hoinka, M. Lingham, P. Hannaford, and C. J. Vale, Phys. Rev. Lett. **106**, 105304 (2011); H. Hu, Phys. Rev. A **84**, 053624 (2011); A. T. Sommer, L. W. Cheuk, M. J. H. Ku, W. S. Bakr, and M. W. Zwierlein, Phys. Rev. Lett. **108**, 045302 (2012); A. M. Fischer and M. M. Parish, Phys. Rev. A **88**, 023612 (2013); V. Makhalov, K. Martiyanov, and A. Turlapov, Phys. Rev. Lett. **112**, 045301 (2014); U. Toniolo, B. C. Mulkerin, C. J. Vale, X.-J. Liu, and H. Hu, arXiv:1701.08477.
[85] J. I. Kapusta and C. Gale, *Finite-Temperature Field Theory: Principles and Applications* (Cambridge University Press, Cambridge, 2006).